RESEARCH ARTICLE

Check for updates

3D QSAR-based design and liquid phase combinatorial synthesis of 1,2-disubstituted benzimidazole-5-carboxylic acid and 3-substituted-5H-benzimidazo[1,2-d][1,4]-benzodiazepin-6(7H)-one derivatives as anti-mycobacterial agents†

Nikum D. Sitwala,[a] Vivek K. Vyas,[a] Piyush Gedia,[a] Kinjal Patel,[a] Rania Bouzeyen,[bc] Saqib Kidwai,[d] Ramandeep Singh[d] and Manjunath D. Ghate (iD) *[a]

Tuberculosis (TB) is one of the world's deadliest infectious diseases, caused by *Mycobacterium tuberculosis* (*Mtb*). In the present study, a 3D QSAR study was performed for the design of novel substituted benzimidazole derivatives as anti-mycobacterial agents. The anti-tubercular activity of the designed compounds was predicted using the generated 3D QSAR models. The designed compounds which showed better activity were synthesized as 1,2-disubstituted benzimidazole-5-carboxylic acid derivatives (series 1) and 3-substituted-5H-benzimidazo[1,2-d][1,4]benzodiazepin-6(7H)-one derivatives (series 2) using the liquid phase combinatorial approach using a soluble polymer assisted support (PEG5000). The compounds were characterized by ^{1}H-NMR, ^{13}C-NMR, FTIR and mass spectrometry. HPLC analysis was carried out to evaluate the purity of the compounds. We observed that the synthesised compounds inhibited the growth of intracellular *M. tuberculosis* H$_{37}$Rv in a bactericidal manner. The most active compound **16** displayed an MIC value of 0.0975 μM against the *Mtb* H$_{37}$Rv strain in liquid cultures. The lead compound was also able to inhibit the growth of intracellular mycobacteria in THP-1 macrophages.

Introduction

According to the WHO, tuberculosis (TB) is a global health burden. It is estimated that one-third of the world's population is infected with the causative agent, *Mycobacterium tuberculosis* (*Mtb*).[1] According to the WHO, each year 10–12 million individuals are diagnosed as new TB patients and this disease is a leading cause of death in adults.[2] The current TB regimen has high toxicity and needs to be administered for an extended duration of 6–9 months.[3] The emergence of drug resistant strains, including multi- and extensively drug resistant TB (MDR-TB and XDR-TB), is making this pandemic more threatening.[4,5] In order to tackle the problem of drug-resistance, there is a need to identify new drug targets and scaffolds with a novel mechanism of action. Benzimidazole analogues have been previously reported as antitubercular agents.[6–9] Benzimidazole derivatives are ionisable, polar, aromatic compounds, and possess antimicrobial activities.[10,11] Substituted-[1,2,3] triazoles along with fluorine have been shown to be very potent antitubercular agents against *Mtb* H$_{37}$Rv. Researchers from Southern Research Institute have identified several benzimidazole, pyridopyrazine and pteridine based tubulin inhibitors with potent antitubercular activity. These molecules such as OTBA, 2-alkoxycarbonylamino-pyridines, 2-carbamoylpteridine, taxanes, benzimidazoles, GTP analogues, benzo[*c*]-phenanthridines, isoquinolines, PC190723, zantrins, and chrysophaentins have been shown to inhibit FtsZ enzymes from *Mtb*.[12–14] Reynolds and others hypothesized that the benzimidazole skeleton, a nitrogen containing heterocycle, represents an important pharmacophore for the development of novel FtsZ inhibitors.[15] In another study, libraries of 2,5,6- and 2,5,7-

[a] *Department of Pharmaceutical Chemistry, Institute of Pharmacy, Nirma University, Ahmedabad 382481, Gujarat, India. E-mail: manjunath.ghate@nirmauni.ac.in*
[b] *Institut Pasteur de Tunis, LTCII, LR11 IPT02, Tunis, 1002, Tunisia*
[c] *Université Tunis El Manar, Tunis, 1068, Tunisia*
[d] *Tuberculosis Research Laboratory, Vaccine and Infectious Disease Research Centre, Translational Health Science and Technology Institute, Faridabad-Gurugram Expressway, Haryana, India*

trisubstituted benzimidazoles were screened against *Mtb* H$_{37}$Rv which resulted in identification of several hit compounds.[16] The selected lead compounds exhibited excellent MIC (the lowest concentration of a synthesised compound which prevented visible growth of *Mtb*) values in the range of 0.39–6.1 μg mL^{-1} against both drug-sensitive and resistant strains. The prediction of drug-like activity has been established by a versatile tool such as QSAR. These techniques are proficient for exclusion of the undesired properties and result in an early prediction of drug-like candidates.[17] A series of molecules can be synthesized by employing the liquid phase combinatorial synthesis approach which is extensively applied for the isolation of multiple targets which could be selected for certain pharmacological evaluation.[18]

In the present study, a 3D QSAR study was performed on tri-substituted benzimidazoles for the design of novel derivatives. 3D QSAR is a quantitative mathematical relationship study, which correlates the biological activity of a series of compounds with their properties calculated in 3D space. We performed comparative molecular field analysis (CoMFA) and comparative molecular similarity indices analysis (CoMSIA) in the 3D QSAR study. Statistical results of CoMFA and CoMSIA were obtained using the partial least squares (PLS) method. PLS is an iterative multivariate regression method, which is able to interpret the effect of chemical structure (independent variable) on biological activity (dependent variable).[17] We used the liquid phase combinatorial synthesis method for the synthesis of designed substituted benzimidazole compounds. The purity of the compounds was evaluated by HPLC and they were characterized by mass spectrometry, FTIR, ^{1}H-NMR and ^{13}C-NMR analysis. In this study, we have also reported the single crystal XRD pattern of one of the potent compounds. The synthesized compounds were non-cytotoxic and also able to inhibit *Mtb* growth *in vitro* and in macrophages. Overall, the combination of QSAR and liquid phase combinatorial synthesis resulted in identification of small molecules that possessed anti-tubercular activity.

Results and discussion

3D QSAR study

The results of PLS analysis are shown in Table S2 in the ESI.† PLS analysis indicated a q^2 value (leave-one-out) of 0.727 and 0.640 for the CoMFA and CoMSIA models, respectively, with a maximum number of 6 latent variables and a SEE (standard error of estimation) value of 0.176 and 0.152 in conjunction with an F (F-test value) value of 161 and 132 for the CoMFA and CoMSIA models, respectively. The QSAR model demonstrated good predictive ability with an r^2_{pred} (predictive correlation coefficient) value of 0.714 and 0.748 for the CoMFA and CoMSIA models, respectively. Plots of experimental pMIC along with predicted pMIC are shown in Fig. S2 in the ESI.†

Contour map analysis

CoMFA contour maps are displayed as steric and electrostatic fields and shown in Fig. S3(A) in the ESI.† CoMSIA contour

maps are shown in Fig. S3(B) in the ESI.† As shown in Fig. S3,† 80% contribution for favourable and 20% contribution for unfavourable field regions for all the contour maps were observed. The most active molecule (**Tr5**) is inserted in all the maps. CoMFA contour maps are shown in green coloured contour (sterically favoured) and yellow coloured contour (sterically unfavoured) regions. A yellow coloured contour was observed just next to the carboxamide functional group, which demonstrated that the presence of a sterically bulky group in this region might result in lowered efficacy; however the green coloured contour at the terminal end of the butoxy group indicated that the introduction of sterically bulky groups may increase the potency of the designed compounds (Fig. S3(A) in the ESI†). Likewise, the C6-position of the benzimidazole ring was also highlighted as the green contour area, which indicated that the introduction of steric groups might lead to the enhancement of efficacy. Electrostatic contour maps (Fig. S4(B)†) are shown in red coloured (electronegative group favoured) and blue coloured contour (electropositive group favoured) regions. The overlap of blue contours for aliphatic substitutions at the C6-position demonstrated that electron donating groups might result in improved efficacy. Also, the presence of adjacent red contours indicated that the existence of electronegative groups would be critical for the design of compounds with better activity. Another red coloured contour at the C5-position indicated that the substitutions of electron withdrawing groups may be essential for good potency of designed compounds. The CoMSIA hydrophobic contour map is shown in Fig. S4(A) in the ESI.† In the CoMSIA hydrophobic contour map, regions favouring hydrophobic substitutions were indicated by yellow contours, whereas regions favouring hydrophilic substitutions were indicated by grey contours. The presence of hydrophobic substitutions such as –CH$_3$, –CH$_2$CH$_3$, –CH$_2$CH$_2$CH$_3$, and –CH(CH$_3$)$_2$ close to the C6-position of the heterocyclic ring (highlighted in yellow contours) resulted in higher efficacy of the compounds. Moreover, substitution with aromatic hydrophobic groups at the C6 position also resulted in good inhibitory activity. The oxygen atoms of carbonyl functionalities such as amides, ureas and carbamates were highlighted by grey contours. Cyan contours indicated the hydrogen bond donor (HBD) favoured regions, whereas HBD disfavoured regions are shown in purple coloured contours (Fig. S4(B) in the ESI†). The hydrogen bond acceptor (HBA) favourable regions are depicted by magenta coloured contours, and the HBA disfavoured regions are shown in red coloured contours (Fig. S4(C) in the ESI†). The cyan coloured contour at the C5-position near the amide bond and the adjacent red contours in the same proximity indicated that the hydrogen bond donating groups at this position might be critical for the biological efficacy associated with this series.

The importance of carbonyl and adjacent substitutions for ureas, amides and carbamates as HBDs in all the molecules is indicated as these functional groups overlap with the cyan contours. Meanwhile, the nitrogen of the benzimidazole ring at the C3-position overlaps with magenta contours, which

indicated that it contributed as a hydrogen bond acceptor, and the same is witnessed in all the molecules. The presence of purple contours specified the need for a hydrogen bond acceptor (HBA) atom as perceived in derivatives with carbamates, which demonstrated higher efficacy in comparison to derivatives with amides. Almost similar observations were achieved whilst taking into consideration the CoMSIA steric and electrostatic contour maps as compared to the CoMFA steric and electrostatic contour maps; however the blue contour at the C1-position suggested that the introduction of electron withdrawing functionalities might cause lower potency, which suggested that the substitution of electron donating groups or sterically bulky groups for the design of new compounds can be taken into consideration for the first position.

Design of molecules

The compounds were designed on the basis of the 3D QSAR study (Fig. 1). We designed 1,2-disubstituted benzimidazole-5-carboxylic acid derivatives as series 1 (30 compounds) and 3-substituted-5H-benzimidazo[1,2-d][1,4]benzodiazepin-6(7H)-one derivatives (22 compounds) as series 2. In both series, the benzimidazole ring was maintained as the main scaffold. We hypothesized that replacing substitutions at the C5-position consisting of carbamates, amides and ureas with methyl ester or carboxylic acid derivatives might result in compounds with better activity. As evident from the contour maps, the increase in activity would be due to characteristics such as electronegativity, hydrophobicity, and HBD and HBA abilities. Furthermore, we diversified the substitutions at the C2-position of the benzimidazole ring system. We also substituted the C1-position of the benzimidazole ring system with a bulky group as per the interpretations from all of the contour map analyses. The anti-mycobacterial activity (pMIC) of the designed compounds were predicted using the generated CoMFA and CoMSIA models (Table S3 in the ESI†) in order to scrutinise the compounds for the synthesis and activity.
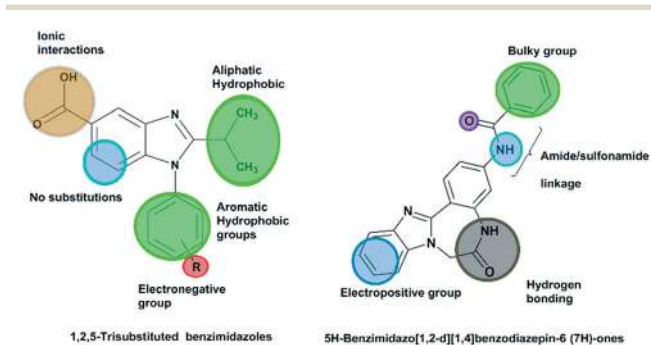

Fig. 1 Design strategy for the design of 1,2-disubstituted benzimidazole-5-carboxylic acid and 5H-benzimidazo[1,2-d][1,4]benzodiazepin-6(7H)-one derivatives using the 3D QSAR generated CoMFA and CoMSIA contour maps.
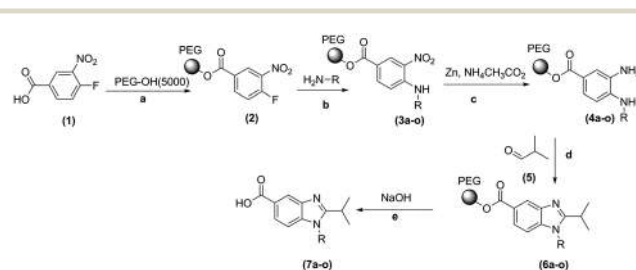
Chemistry

Scheme 1 describes the synthesis of 1,2-disubstituted benzimidazole-5-carboxylic acid derivatives (series 1) and Scheme 2 describes the synthesis of 3-substituted-5H-benzimidazo[1,2-d][1,4]benzodiazepin-6(7H)-one derivatives.
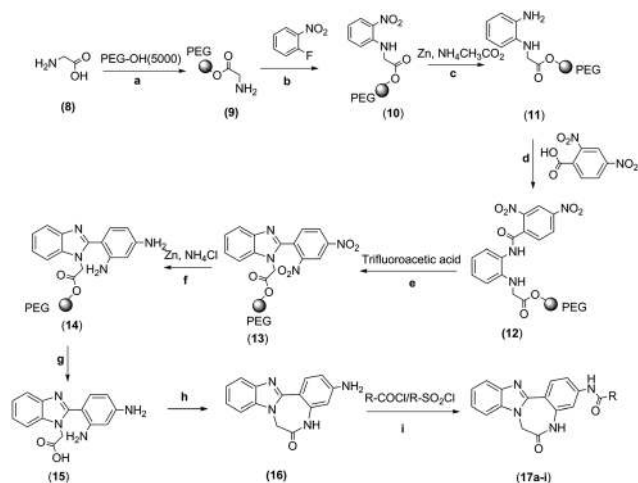
Series 1

A soluble polymer support-based liquid phase combinatorial synthesis method was used, in which PEG5000 mono methyl ether was utilized as the polymer attachment to synthesize compounds 7a–o. After a wide range of route investigations and evaluations of all applicable variations for all intermediates synthesized including the use of different reaction conditions, catalysts, temperatures, reagents, etc., various benzimidazole derivatives were synthesized.[18–20] The resulting procedures involved coupling 3-nitro-4-flouro-benzoic acid (1) with PEG using 1-ethyl-3-(3-dimethylaminopropyl)-carbodiimide as a reagent for amide formation along with dimethylaminopyridine (DMAP) as a catalyst in dichloromethane (DCM). Precipitation of the polymer bound derivative was performed using cold diethyl ether and the solid was filtered and washed using ether to achieve pure polymer bound 3-nitro-4-fluoro benzoic acid (2).[21,22] Introduction of various substituted amines in the following step was depicted by activated fluoro due to the presence of a nitro group at 25 °C to obtain PEG coupled substituted o-nitroamine (3a–o) derivatives. Diethyl ether was added to obtain solid PEG coupled o-nitroanilines which were filtered and unreacted reagents were removed by washing.

The purity of the compounds (3a–o) was verified by TLC analysis. A mixture of ammonium acetate and zinc at 25 °C was added to reduce the aromatic nitro group to amine. After completion of the reduction reaction, the reaction mixture was filtered to remove the inorganic salts and diamine derivatives (4a–o) were precipitated upon addition of diethyl ether and isolated.[18] The next step involved the use of isobutraldehyde (5) to react with diamine derivatives (4a–o) to obtain intermediate substituted benzimidazoles (6a–o).[23] In the concluding step, a solution of sodium hydroxide in methanol was used for cleavage of PEG to form the final desired benzimidazole derivatives (7a–o). The chemical structure of

Scheme 1 Synthetic scheme for the synthesis of 1,2-disubstituted benzimidazole-5-carboxylic acid derivatives using the liquid phase combinatorial synthesis technique. Reagents and conditions: (a) DCM, EDC, DMAP 0 °C to rt; (b) DCM, rt; (c) MeOH, rt; (d) THF, reflux; (e) MeOH, rt.

This journal is © The Royal Society of Chemistry 2019

Med. Chem. Commun., 2019, **10**, 817–827 | 819

Scheme 2 Synthetic scheme for the synthesis of 5*H*-benzimidazo[1,2-*d*][1,4]benzodiazepin-6(7*H*)-one derivatives using the liquid phase combinatorial synthesis technique. Reagents and conditions: (a) DCM, EDC, DMAP 0 °C to rt; (b) DCM, rt; (c) MeOH, rt; (d) DCM, DMAP, EDC, rt; (e) MgSO$_4$, DCE reflux (f) MeOH, rt; (g) NaOH; (h) DCM, DMAP, EDC to rt; (i) TEA.

all the synthesized compounds was verified by various analytical procedures such as mass spectrometry, ^{1}H-NMR along with D$_2$O exchange, ^{13}C-NMR, FTIR spectroscopy (ESI†). In this series of molecules, important features are observed in the FT-IR spectra of molecules **7a–o**, which revealed typical carbonyl (acid) stretching peaks around 1830–1810 cm^{-1}, aromatic C–H stretching peaks near 3045–3010 cm^{-1}, aliphatic C–H stretching peaks near 2970–2930 cm^{-1} and carboxylic acid stretch ranging from 3300–2950 cm^{-1} (ESI†). For all the molecules, M + 1 peaks as stable base peaks were observed in all mass spectra (ESI†). A JASCO 4000 HPLC with a C18 column (250 mm × 4 mm) was used to analyse the purity of the compounds; mobile phase methanol : 0.1% formic acid aqueous buffer (60 : 40) as an isocratic system with 15 minutes runtime and 1 ml per minute flow rate was used for all the derivatives and the results indicated purity >95% for each compound (ESI†). Moreover, all HPLC data were validated using peak purity analysis by overlay of UV graphs and each desired peak demonstrated high peak purity. In ^{1}H NMR spectra, substantial features were observed for all the compounds. Two peaks of aliphatic protons of isopropyl substitution at the C2 position of the benzimidazole ring appeared as a doublet at 1.6 ppm and as a multiplet at 4.8 ppm, along with aromatic protons mostly observed as multiplets at 6.7–8.0 ppm. Furthermore, the protons of carboxylic acid demonstrated a broad peak at approximately 13 ppm for all the compounds, which got exchanged after D$_2$O addition. Similarly, the 2 peaks of aliphatic carbons of isopropyl substitution at the 2nd position of the benzimidazole ring appeared at 21 ppm and 48 ppm in the ^{13}C NMR spectra for all the of molecules along with sets of aromatic carbons observed from 120–140 ppm. Furthermore, the carbons of carboxylic acid demonstrated a peak at approximately 165 ppm for all the compounds (ESI†). The crystal structure of compound **7a** was

derived using single crystal X-ray diffraction analysis and is shown in Fig. S5 in the ESI† with details of the single crystal study.

Series 2

Scheme 2 describes the synthesis of compounds **17a–i** *via* implementation of the soluble polymer support PEG5000 mono methyl ether and reactions based on the liquid phase combinatorial synthesis approach.

Final synthetic procedures were adopted in which glycine (**8**) was reacted with PEG using 1-ethyl-3-(3-dimethylaminopropyl)carbodiimide (EDC) as a reagent for ester formation along with DMAP as a catalyst in EDC.[22] The PEG coupled glycine (**9**) was purified by filtering the reaction suspension obtained upon addition of diethyl ether followed by excess addition of diethyl ether to rinse the solid and vacuum dried. ^{1}H-NMR was conducted to evaluate the purity of compound **9**.[23] In the next step, the amine of derivative **9** was reacted with 1-fluoro-2-nitrobenzene at 25 °C to obtain intermediate **10**. The *o*-nitroaniline derivative was further purified by filtration of the suspension obtained upon addition of diethyl ether. The purity of compound **10** was verified by ^{1}H-NMR. Ammonium acetate and zinc were mixed and used at 25 °C to obtain the amine derivative from the reduction of nitro derivatives, and after stirring in the solvent completion of the reaction was observed. Additionally, the diamino derivative (**11**) was further purified upon filtration of the suspension obtained by the addition of cold diethyl ether. The diamino substituted derivative (**12**) was obtained upon reacting **11** with 2,4-dinitrobenzoic acid, which upon cyclization in the presence of magnesium sulphate and trifluoroacetic acid formed the substituted benzimidazole derivative (**13**).[22] Reduction of the dinitro derivative was achieved by the addition of ammonium acetate and zinc at 25 °C which were precipitated using diethyl ether to purify the diamino derivative (**14**). In the next step, a methanolic solution of sodium hydroxide was used to get the carboxylic acid derivative (**15**).[18] This intermediate was further reacted in the presence of EDC/DMAP to obtain the cyclized product as the core fused ring structure (**16**). In the final synthetic step, the reaction of the amine derivative (**16**) with various acid chlorides and sulphonyl chloride was performed using TEA as a base and various derivatives were obtained (**17a–i**).[20] The chemical structures of all the synthesised compounds were established using mass spectrometry, FT-IR, ^{1}H-NMR along with D$_2$O exchange, and ^{13}C-NMR spectral analysis. The synthesized molecules demonstrated M + 1 peaks in the mass spectrum corresponding to all the molecules respectively. Compounds **17a–i** revealed typical amidic N–H stretching peaks near 3350–3275 cm^{-1}, aliphatic C–H stretching peaks near 2960–2920 cm^{-1} and C=O stretching peaks near 1725–1700 cm^{-1}, whereas compound **16** along with the above mentioned peaks also showed an –NH$_2$ doublet peak in the range of 3350–3250 cm^{-1}. The purity of the compounds was analysed using a JASCO 4000 HPLC with a C18 column (250 mm × 4 mm) and mobile phase methanol :

0.1% formic acid aqueous buffer (80 : 20) as an isocratic system with 10 minutes run time and 1 ml per minute as the flow rate; all the molecules illustrated purity (>95%). The significant feature of the ^{1}H NMR spectra of the compounds was observed as the aliphatic region displaying 2 protons at the C1 position of the benzimidazole ring and these appeared at approximately 4.8 ppm for all the tested compounds. Furthermore, compound 16 showed 2 amine protons at approximately 5.8 ppm, and these protons were absent in amide derivatives 17a–i. The amide derivatives demonstrated an amide peak at approximately 10.5 ppm along with sets of aromatic protons in the range of 6.5–8.5 ppm for all the compounds. Also, upon D_2O analysis the exchangeable protons including –NH$_2$ for 16 and amidic for 17a–i got exchanged. The significant feature of the ^{13}C NMR spectra for this series of molecules was detected as the peaks of aliphatic carbon of fused ring substitution at the C2 position of the benzodiazepine ring appearing at 46 ppm. Furthermore, the carbons of amide demonstrated a peak at approximately 168 ppm for all the compounds. The carbons of the aromatic ring displayed peaks in the range of 120–140 ppm.

Pharmacological activity

***In vitro* antitubercular activity.** All the synthesized substituted benzimidazole derivatives of series 1 (1,2-disubstituted benzimidazole-5-carboxylic acid) and series 2 (3-substituted-5H-benzimidazo[1,2-d][1,4]benzodiazepin-6(7H)-one derivatives) were evaluated for *in vitro* antitubercular activity against *Mtb* H$_{37}$Rv using MIC determination assays. The results of antitubercular activity analysis of all the synthesized compounds along with the standard drug isoniazid (INH) are reported in Table 1. Most of the synthesized compounds of both series exhibited good *in vitro* antimycobacterial activity. In series 2, compound 16 was the most active compound with an MIC value of 0.0975 μM against *Mtb* H$_{37}$Rv. Other compounds *viz.* 17d, 17e, 17h, 7e and 7f also displayed decent activity against *Mtb* H$_{37}$Rv with MIC values of 1.56 μM, 0.19 μM 0.78 μM, 0.78 μM and 0.78 μM, respectively.

Macrophage results (cellular cytotoxicity). We next determined the cellular cytotoxicity of the active compounds against THP-1 macrophages using the WST-1 cell viability kit. We observed that 16, 17d, 17e, 17h, 7e, and 7f were non-cytotoxic even at 50 μM concentration (the highest concentration tested in our assays). The remaining two active compounds, 17c and 17g, were non-cytotoxic at 10 μM concentration. Next, we evaluated a few of these non-cytotoxic compounds for their ability to inhibit the growth of intracellular *Mtb* H$_{37}$Rv in a THP-1 model of infection (Fig. 2). As shown in Fig. 2, pre-treatment with these compounds resulted in growth inhibition of *Mtb* in THP-1 macrophages. The exposure of THP-1 to 16, 17c, 17d, 7e, and 7f resulted in approximately 8.0–10.0 fold reduction in bacterial counts, in comparison to untreated cells at day 4 post-infection (Fig. 2, ***P < 0.001). As expected, the maximum inhibition of intra-

cellular growth (30.0 fold) was observed in THP-1 macrophages treated with INH for 4 days (Fig. 2, ***P < 0.001).

Structure–activity relationship (SAR). The aliphatic functional group at the C1-position of the benzimidazole ring is important for activity as the second series of compounds (3-substituted-5H-benzimidazo[1,2-d][1,4]benzodiazepin-6(7H)-one derivatives) (16, 17a–i) exhibits better activity as compared to the first series of compounds (1,2-disubstituted benzimidazole-5-carboxylic acid derivatives) (7a–o). In the first series, the bulky groups at the C1-position of the benzimidazole ring might cause steric hindrance towards the binding of compounds with their cellular target. Moreover, the lipophilicity of both series of compounds was comparable due to the presence of aromatic rings. The lipophilicity of molecules would result in easy permeability for the compounds across *Mtb* cells. The presence of a free amine group (unsubstituted) at the C9-position in 16 (MIC = 0.0975 μM) resulted in the best activity as compared to the substituted derivatives (17a–i). The presence of an amide spacer between the benzimidazole ring and –R substitution (terminal aromatic ring derivative) *viz.* 17g (MIC = 0.39 μM) showed a 4.0 fold better activity as compared to the sulphonamide spacer in 17i (MIC = 1.56 μM). Interestingly, compounds with a phenylfluoro functional group such as 17e (MIC = 0.195 μM) displayed better activity as compared to compounds with phenylbromo substitutions such as 17b (MIC = >50 μM). Despite both being electronegative atoms, fluoro would improve the lipophilicity, and this might be responsible for the better activity. We also observed that the presence of an amide functional group in the cyclized ring at the C1-position of the benzimidazole ring throughout the second series of compounds is also crucial for the activity. We observed that compound 7e (MIC = 0.78 μM), with the hydroxyl functional group in series 2 in a similar spatial arrangement, showed better activity as compared to the remaining compounds in series 1. Moreover, while comparing 7e and 7g (MIC = 25 μM), we observed a drastic reduction in the potency upon the change in the position of the hydroxyl and methoxy groups. These results indicated that the presence of HBD groups at this position is crucial for *in vitro* biological activity. Furthermore, introduction of an aliphatic long chain spacer in compounds 7m (MIC = 50 μM), 7n (MIC = 50 μM), and 7o (MIC = 25 μM) did not significantly improved the potency of the compounds. Taken together, we concluded that an amide or hydroxyl group (hydrogen bond donor) at one or two carbon length is important for the observed activity. The presence of an amine group at the C9-position is also vital for the enhanced activity of these molecules. Furthermore, the presence of substitutions that increase the lipophilicity of the compounds also resulted in better biological activity. We also demonstrated that introduction of one carbon longer spacer at the C1-position resulted in lower potency of the compounds and sulphonamide spacer derivatives showed lower activity in comparison to compounds with an amide spacer.

In the following sub-section, we made a comparison of this study with recently published papers on benzimidazoles

Table 1 Structures and *in vitro* antitubercular activity of 1,2,5-trisubstituted benzimidazole (series 1) and 3-substituted-5*H*-benzimidazo[1,2-*d*][1,4]benzodiazepin-6(7*H*)-one (series 2) derivatives (MIC, μM) against *Mtb* H37Rv
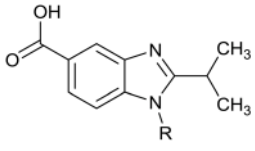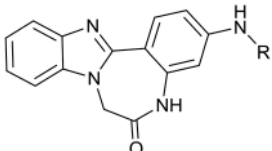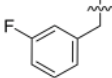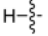

(7a-o)
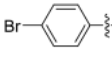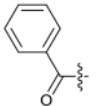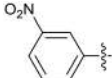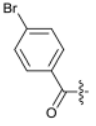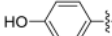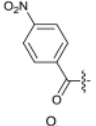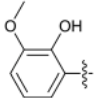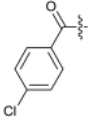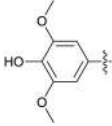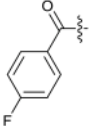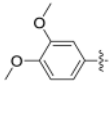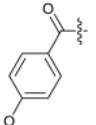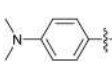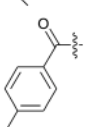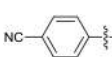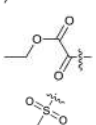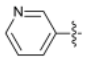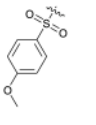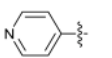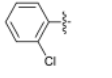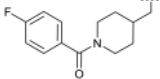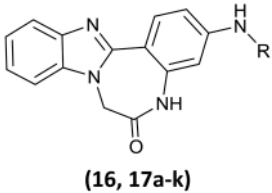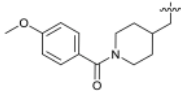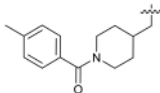
(16, 17a-k)

Compounds	R	MIC (μM)	Compounds	R	MIC (μM)
7a		12.5	16		0.0975
7b		50	17a		>50
7c		25	17b		>50
7d		50	17c		0.195
7e		0.78	17d		1.56
7f		0.78	17e		0.195
7g		25	17f		3.125
7h		50	17g		0.39
7i		50	17h		0.78
7j		50	17i		1.56
7k		25	Isoniazid (INH)		0.39
7l		>50			
7m		50			

822 | *Med. Chem. Commun.*, 2019, **10**, 817–827

This journal is © The Royal Society of Chemistry 2019

Table 1 (*continued*)

(7a-o)   **(16, 17a-k)**

Compounds	R	MIC (μM)		Compounds	R	MIC (μM)
7n		50				
7o		25				

with anti-mycobacterial activity and QSAR study. Picconi *et al.*[10] synthesized novel triaryl benzimidazoles and evaluated them against multi-drug resistant (MDR) Gram-positive and Gram-negative species. 2-Methyl-1-(5-{3-[(2-methyl-3*H*-benzoimidazole-5-carbonyl)-amino]-phenyl}-pyridin-2-yl)-1*H*-benzoimidazole-5-carboxylic acid(3-dimethylamino-propyl)-amide (**18**) demonstrated MICs in the range of 16–32 μg mL^{-1} against Gram-positive and Gram-negative species. Ashok *et al.*[24] synthesized indole-tethered benzimidazole-based 1,2,3-triazoles using conventional and microwave-assisted synthesis and evaluated them for anti-mycobacterial, antioxidant and antimicrobial activities. 2-(1-((1-(2-Nitrophenyl)-1*H*-1,2,3-triazol-4-yl)methyl)-1*H*-indol-3-yl)-1*H*-benzo[*d*]imidazole
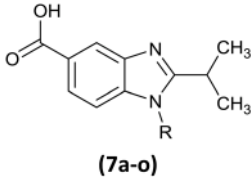
(**19**) (Fig. 3) showed an MIC value of 3.125 μg mL^{-1} against *Mtb* H$_{37}$Rv which is less potent as compared to that of **16** (MIC = 0.0975 μM). Compound **19** was predicted with a clog*P* value of 2.38, and showed a drug likeness value of −5.47. Compound **16** showed a clog*P* value of 1.78 and a drug likeness value of 2.97. Chaturvedi *et al.*[25] reported the synthesis of 2-arylbenzimidazoles in a molecular sieve–MeOH system and evaluated them for antitubercular activity. The synthesized compound **20** (Fig. 3) showed an MIC value of 16 μM against *Mtb* H$_{37}$Rv and was predicted with a log*P* value of 4.45. This compound is less potent in comparison with **16** (MIC = 0.0975 μM, log*P* = 0.78). Yoon *et al.*[26] synthesized new benzimidazole aminoesters and evaluated them for antimycobacterial activity. Ethyl 2-(4-(trifluoromethyl)phenyl)-1-(2-morpholinoethyl)-1*H*-benzo[*d*]imidazole-5-carboxylate (**21**) (Fig. 3) was found to be the most active with an IC$_{50}$ of 11.52 μM. Chandrasekera *et al.*[27] synthesized novel phenoxyalkylbenzimidazoles (PAB) (**22**) (Fig. 3) with improved
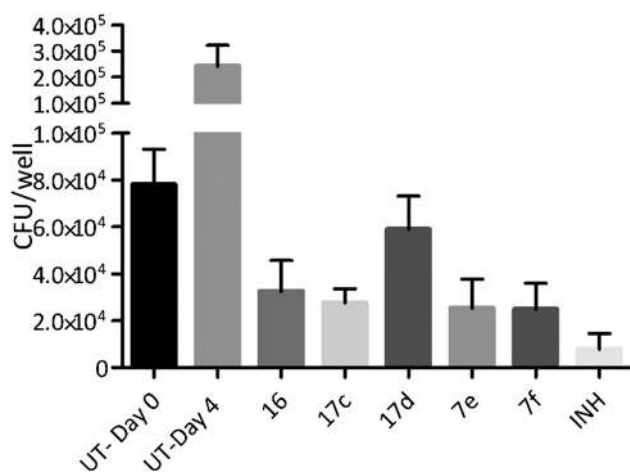
Fig. 2 Activity of identified synthesized compounds (**16**, **17c**, **17d**, **7e** and **7f**) against intracellular *Mtb* in macrophages: THP-1 macrophages were infected with *Mtb* at a MOI of 1 : 10. Following 24 h of infection, cells were overlaid with RPMI medium containing the synthesized compounds (**16**, **17c**, **17d**, **7e** and **7f**). After incubation for 4 days, macrophages were lysed in 1 ml of 1× PBS–0.1% Triton X-100 and 100 ml of 10.0 fold serial dilutions were plated on MB7H11 plates at 37 °C for 3–4 weeks. The data shown in this panel are mean + S.E. obtained from triplicated wells. Significant differences were obtained for the indicated groups. **$p < 0.01$ and ***$p < 0.001$.
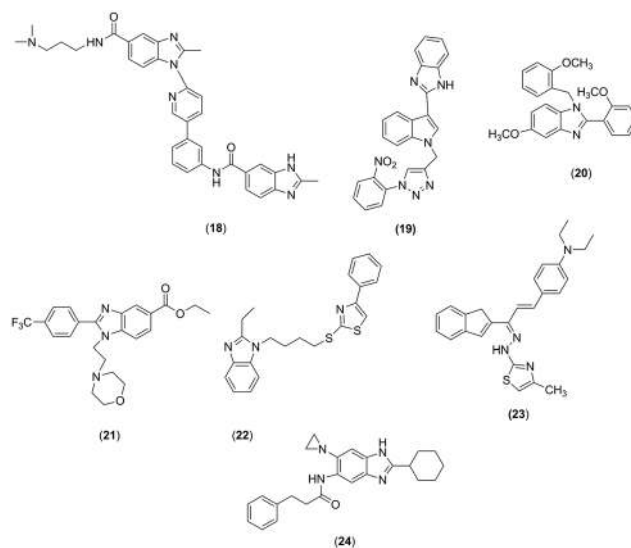
Fig. 3 Benzimidazoles (**18**–**24**) reported as anti-mycobacterial agents.

activity against *Mtb*. The authors suggested that the discovery of the PAB compounds allowed them to design and discover novel compounds which can target intracellular *Mtb*. The most potent compounds showed inhibitory concentrations against *Mtb* in the low nanomolar range. Surineni *et al.*[28] synthesized benzimidazole tethered allylidenehydrazinylmethylthiazole derivatives as potent inhibitors of *Mtb*. The authors suggested that compound **23** (Fig. 3) is a lead compound of the series which could be further optimized development of novel and effective antitubercular agents. Compound **23** showed an MIC$_{90}$ value of 2.5 µg mL^{-1} and was predicted with a clog*P* value of 6.22 and a log*P* value of 6.03. Ahamad *et al.*[29] performed 2D and 3D QSAR, molecular docking and MD simulation studies on substituted benzimidazole derivatives targeting the FtsZ protein of *Mtb.* The results of the 3D QSAR study suggested the importance of both electrostatic and steric descriptors in determining the activity of benzimidazole derivatives. Based on the QSAR study, the authors designed 223 new benzimidazole derivatives and performed *in silico* ADMET analysis and docking study. The authors concluded that the designed compound **24** (log*P* = 4.57) (Fig. 3) was found to be the most potent among all the designed compounds with better *in silico* results as compared with the reported compounds used in the QSAR study.

Experimental

3D QSAR analysis

Sybyl X molecular modeling software (Tripos Inc., St. Louis, MO) was used to perform the 3D QSAR study. The 3D QSAR study was performed on previously reported 70 benzimidazole derivatives (Table S1 in the ESI†).[16,19,20] The compounds were screened for *Mtb* H$_{37}$Rv inhibition, and values of MIC were reported in the micromolar range. The activity value (MIC) was converted into the logarithm based scale and used as a dependent variable (pMIC = −log MIC) in the 3D QSAR study. The data set of 70 compounds was divided into test set (Ts) comprising 25 molecules and training set (Tr) comprising 45 molecules. Alignment of molecules was achieved by a pharmacophore-based alignment method as shown in Fig. S1 in the ESI.† Pharmacophore based alignment was executed using the DISCOtech module of sybyl X. CoMFA fields (steric and electrostatic) were calculated for each training and test set of compounds using sp^3 hybridized carbon as the probe atom using Lennard-Jones potential and Coulomb potential, respectively, and used as independent variables. CoMSIA similarity index descriptors were calculated using the same default parameters as CoMFA. Statistical analysis was performed using the PLS regression method.

Chemistry

Scientific MP1 melting point apparatus was used to record the melting point range for all the synthesized molecules and the uncorrected melting points are reported. Refluxing and stirring of reaction mixtures were done using a REMI rotamantle and magnetic stirrers. The synthesized derivatives and final molecules were dried using an IR lamp and vacuum desiccator. A JASCO FTIR instrument was used to record the FTIR spectra and the KBr dispersion method was used to prepare the samples. An Agilent mass spectrometer employing the electron spray ionization (ESI) technique was used as the ion source for the evaluation of the mass spectra and recording them. A BRUKER ^{1}H NMR 400 MHz instrument was used to record the proton NMR spectra and a BRUKER ^{13}C NMR 100 MHz instrument was used to record the carbon NMR spectra. The chemicals were acquired from Sigma Aldrich, Alfa Aesar, TCI and Spectrochem and experimental protocols were performed in fume hoods.[18]

Synthesis of 1,2-disubstituted benzimidazole-5-carboxylic acids (series 1)

General procedure for synthesis of 4-fluoro-3-nitrobenzoate PEGester (2) (Scheme 1). 1-Ethyl-3-(3-dimethylaminopropyl)carbodiimide (EDC) (0.61 g, 2.97 mmol) was added at 5 °C to a stirred mixture of PEG-5000 mono methyl ether (13.51 g, 2.7 mmol) and 4-fluoro-3-nitrobenzoic acid (**1**) (0.5 g, 2.7 mmol) in dichloromethane (DCM) (100 ml). After 15 minutes of additional stirring, 4-dimethylaminopyridine (DMAP) (0.033 g, 0.27 mmol) was added at 5 °C. The reaction mixture was slowly brought to 25 °C and stirred for 12 h. The progression of the reaction was examined by TLC (mobile phase used: 70% ethyl acetate in petroleum ether). The solution was filtered and the filtrate was added to cold diethyl ether. The suspension obtained was vacuum filtered to obtain the crude intermediate 2. Purification was not performed, and the product obtained was used in the next step.[18]

General procedure for synthesis of 4-amino substituted-3-nitro-benzoate PEGester (3a–o). The substituted amines (2.0 eq.) were added at 25 °C to a solution of intermediate 2 (10.0 g, 1.94 mmol) in DCM (50 ml). Further, stirring of the resulting solution was continued for 16 h at 25 °C.[21,22] The progression of the reaction was examined by TLC (mobile phase used: 80% ethyl acetate in petroleum ether). The reaction mixture was added to cold diethyl ether. The resulting solids were filtered to give the crude intermediates 3a–o, purification was not carried out and the products obtained were used in the next step.

General procedure for synthesis of 4-aminosubstituted-3-amino-benzoate PEGester (4a–o). Ammonium acetate (0.407 g, 7.6 mmol) and zinc (0.292 g, 4.56 mmol) were added at 25 °C to a solution of intermediates 3a–o (8.0 g, 1.52 mmol) in methanol (40 ml). The resulting suspension was further stirred for 16 h at 25 °C.[21] The completion of the reaction was examined by TLC. The reaction suspension was filtered to remove unreacted starting materials and the filtrate was added to cold diethyl ether. The suspension thus obtained was vacuum filtered to isolate the desired intermediates 4a–o, purification was not carried out and the products obtained were used in the next step.

General procedure for synthesis of 2-isopropyl-1-substituted-benzimidazole-5-carboxylate PEGester (6a–o). Isobutyraldehyde (5) (1.6 mmol) was added at 25 °C to a solution of intermediates 4a–o (7.0 g, 1.34 mmol) in tetrahydrofuran (THF) (35 ml). The reaction mixture was further stirred at 80 °C.[23,30–32] The progression of the reaction was examined by TLC (mobile phase used: 5% methanol in chloroform) and the desired product was formed after 7 h of stirring at 90 °C. The reaction mixture was added to cold diethyl ether. The suspension thus obtained was vacuum filtered to isolate the desired intermediates (6a–o).

General procedure for synthesis of 1,2-disubstituted benzimidazole-5-carboxylic acid derivatives (7a–o). Sodium hydroxide (2 eq.) was added at 5 °C to a solution of intermediates 6a–o (1 eq.) in methanol (40 ml). After 15 minutes of additional stirring, the reaction mixture was removed from the ice bath and stirred at 25 °C for 24 h.[33–35] The progression of the reaction was examined by TLC (mobile phase used: 10% methanol in chloroform) which showed that the desired products were formed after 24 h of stirring at 25 °C. The reaction mixture was added to cold diethyl ether. The resulting solids were filtered under reduced pressure to afford the crude final compounds 7a–o as series 1, which were further purified by column chromatography.

Synthesis of 5H-benzimidazo[1,2-d][1,4] benzodiazepin-6(7H)-one derivatives (series 2)

General procedure for synthesis of PEG aminoacetate (9) (Scheme 2). 1-Ethyl-3-(3-dimethylaminopropyl)carbodiimide (EDC) (1.2 eq.) was added at 5 °C to a mixture of PEG-5000 mono methyl ether (1 eq.) and glycine (8) (1 eq.) in dichloromethane (DCM) (50 ml). After 15 minutes of additional stirring, 4-dimethylaminopyridine (DMAP) was added (0.1 eq.) at 5 °C and further stirred for 18 h at 25 °C.[22] The completion of the reaction was examined by TLC (mobile phase used: 80% ethyl acetate in petroleum ether). The desired product was formed after 18 h of stirring at 25 °C. The reaction mixture was filtered and the filtrate was added to cold diethyl ether. The suspension obtained was vacuum filtered to obtain the crude intermediate 9.

General procedure for synthesis of PEG [(2-nitrophenyl)amino]acetate (10). 1-Fluoro-2-nitrobenzene (1 eq.) and triethyl amine (1 eq.) were added at 25 °C to a solution of intermediate 9 (1 eq.) in DCM (50 ml) and stirred for 8 h at 25 °C.[21,22] The progression of the reaction was examined by TLC (mobile phase used: 4% methanol in chloroform) and the desired product was formed after 8 h of stirring at 25 °C. The reaction mixture was added to cold diethyl ether. The suspension obtained was vacuum filtered to obtain the crude intermediate 10.

General procedure for synthesis of PEG [(2-aminophenyl)amino]acetate (11). Ammonium acetate (4 eq.) and zinc (2 eq.) were added at 25 °C to a solution of intermediate 10 (1 eq.) in methanol (40 ml) and the resulting solution was stirred for 6 h at 25 °C.[21] The progression of the re-

action was examined by TLC (mobile phase used: 5% methanol in toluene) and the desired product was formed after 6 h of stirring at 25 °C. The reaction mixture was filtered to remove unreacted zinc and the filtrate was added to cold diethyl ether. The suspension obtained was vacuum filtered to obtain the crude intermediate 11.

General procedure for synthesis of PEG ({2-[(2,4-dinitrobenzoyl)amino]phenyl}amino) acetate (12). EDC (1.2 eq.) was added at 5 °C to a mixture of compound 11 (1 eq.) and 2,4-dinitro benzoic acid (1 eq.) in DCM (50 mL). After 15 minutes of additional stirring, DMAP was added (0.1 eq.) at 5 °C.[23,30–32] Further, stirring of the resulting solution was continued for 12 h at 25 °C. The progression of the reaction was examined by TLC (mobile phase used: 5% methanol in toluene) and the formation of the desired product was observed after 12 h of stirring at 25 °C. The reaction mixture was added to cold diethyl ether. The suspension obtained was vacuum filtered to obtain the crude intermediate 12.

General procedure for synthesis of PEG [2-(2,4-dinitrophenyl)-1H-benzimidazol-1-yl]acetate (13). Magnesium sulphate (1 eq.) was added followed by addition of trifluoro acetic acid (0.2 eq.) at 5 °C to a solution of compound 12 (1 eq.) in DCE (40 ml). Further, stirring of the resulting solution was continued for 6 h under reflux.[22] The progression of the reaction was examined by TLC (mobile phase used: 70% ethyl acetate in hexane) which demonstrated that the starting materials were consumed which resulted in the formation of the desired product after 6 h of stirring under reflux. The reaction mixture was added to cold diethyl ether. The suspension obtained was vacuum filtered to obtain the crude intermediate 13.

General procedure for synthesis of PEG [2-(2,4-diaminophenyl)-1H-benzimidazol-1-yl]acetate (14). Ammonium acetate (4 eq.) and zinc (2 eq.) were added at 25 °C to a solution of intermediate 13 (1 eq.) in methanol (40 ml). The resulting suspension was further stirred for 8 h at 25 °C.[21] The progression of the reaction was examined by TLC (mobile phase used: 5% methanol in chloroform) and the desired product was formed after 6 h of stirring at 25 °C. The reaction mixture was filtered to remove zinc and the filtrate was added to cold diethyl ether. The suspension obtained was vacuum filtered which yielded the crude intermediate 14.

General procedure for synthesis of [2-(2,4-diaminophenyl)-1H-benzimidazol-1-yl]acetic acid (15). Sodium hydroxide (1.5 eq.) was added at 5 °C to a solution of intermediate 14 (1 eq.) in methanol (20 ml). After 15 minutes of additional stirring, the reaction mixture was removed from the ice bath and stirred for 6 h at 25 °C.[21] The progression of the reaction was examined by TLC (mobile phase used: 10% methanol in chloroform) and the desired product was formed after 6 h of stirring at 25 °C. The reaction mixture was added to cold diethyl ether. The suspension obtained was vacuum filtered to obtain the crude carboxylic acid derivative 15.

General procedure for synthesis of amino-5H-benzimidazo[1,2-d][1,4]benzodiazepin-6(7H)-one (16). EDC (1.2 eq.) was added at 5 °C to a solution of compound 15 (1

This journal is © The Royal Society of Chemistry 2019

Med. Chem. Commun., 2019, 10, 817–827 | 825

eq.) in DCM (15 mL). After 15 minutes of additional stirring, DMAP was added (0.1 eq.) at 5 °C.[23,30–32] Further, stirring of the resulting solution was continued for 6 h at 25 °C. The progression of the reaction was examined by TLC (mobile phase used: 5% methanol in toluene) and the desired product was formed after 6 h of stirring at 25 °C. The reaction mixture was added to cold diethyl ether. The suspension obtained was vacuum filtered to obtain the crude intermediate **16**, which was purified by column chromatography.

General procedure for synthesis of substituted amino-5H-benzimidazo[1,2-d][1,4]benzodiazepin-6(7H)-one (17a–i). Triethyl amine (1.5 eq.) was added at 5 °C to a mixture of compound **16** (1 eq.) in DCM (10 ml). After 15 minutes of additional stirring, various substituted acid chloride derivatives were added (1 eq.) at 5 °C. Further, stirring of the resulting solution was continued for 3 h at 25 °C.[20] The progression of the reaction was examined by TLC (mobile phase used: 80% ethyl acetate in hexane) and the desired products were formed after 3 h of stirring at 25 °C. The reaction mixture was added to cold water. The resulting solids were extracted with ethyl acetate (3 × 25 ml) to obtain the crude final compounds as series 2 (**17a–i**). The final compounds were further purified using column chromatography as per standard protocols.

Biological evaluation

***In vitro* antitubercular activity (MIC determination assay).** *Mtb* H$_{37}$Rv was cultured in Middlebrook (MB) 7H9 broth supplemented with 10% albumin dextrose saline, 0.2% glycerol, and 0.05% tween-80 or MB 7H11 agar supplemented with 10% OADS as per standard protocols. For this assay, *Mtb* H$_{37}$Rv was grown in MB 7H9 medium till an OD$_{600nm}$ of 0.2, diluted 1000× and added to 96 well plates containing the synthesized compounds. For MIC determination, 96-well plates were incubated for 14 days as per standard protocols. All the synthesized compounds were prepared in DMSO as 50 mM stock solutions. All the compounds were evaluated for anti-mycobacterial activity in the concentration range of 0.05 to 50 μM. The 96-well plates were incubated at 37 °C for 14 days and determination of MIC values was carried out as per standard protocols.[36]

Evaluation of cytotoxicity and antibacterial activity of synthesized compounds in macrophages. The WST-1 cell proliferation kit was used to perform the cell viability assay as per the manufacturer's recommendations (Sigma Merck, USA). For intracellular killing protocols, THP-1 macrophages were seeded at a density of 2 × 10^5 in 24-well plates and differentiated by the addition of phorbol 12-myristate 13-acetate (PMA) (Sigma Merck, USA). Subsequently, macrophages were infected with *Mtb* at a MOI of 1 : 10. Subsequent 4 h post-infection, removal of extracellular bacteria was performed by overlaying macrophages with RPMI medium containing 200 μg ml^{-1} amikacin for 2 h. After 24 h post-infection, macrophages were washed with 1× PBS and overlaid with RPMI medium containing drugs at non-cytotoxic concentration for 4 days. For bacterial enumeration, macrophages were lysed in 1× PBS–0.1% Triton X-100 and 100 μl of 10.0 fold serial dilutions were plated on MB 7H11 plates at 37 °C for 3–4 weeks.[36]

Conclusions

The present study described the 3D QSAR-based design, synthesis, and *in vitro* antitubercular and intracellular activity of 1,2-disubstituted benzimidazole-5-carboxylic acid and 3-substituted-5H-benzimidazo[1,2-d][1,4]benzodiazepin-6(7H)-one derivatives. We designed and synthesized various substituted benzimidazoles in good yields and evaluated them for anti-mycobacterial activities. Among these, compound **16** exhibited the best *in vitro* antitubercular activity against *Mtb* H$_{37}$Rv in liquid cultures. Compound **16** was also found to be non-cytotoxic in the macrophage assay. Finally, in addition to compound **16**, other compounds **17d**, **17e**, **17h**, **7e** and **7f** also exhibited anti-mycobacterial activity in THP-1 macrophages. Taken together, our screening assays demonstrated that compound **16** is a lead candidate that can be optimized further for design of new antitubercular agents.

Conflicts of interest

There are no conflicts to declare.

Acknowledgements

References

1 A. Koul, E. Arnoult, N. Lounis, J. Guillemont and K. Andries, *Nature*, 2011, **469**, 483–490.
2 WHO, (accessed April 2018).
3 A. A. Velayati, P. Farnia and A. M. Farahbod, *Int. J. Mycobact.*, 2016, **5**, S161.
4 A. Zumla, P. Nahid and S. T. Cole, *Nat. Rev. Drug Discovery*, 2013, **12**, 388–404.
5 M. Schito, D. Hanna and A. Zumla, *Int. J. Infect. Dis.*, 2017, **56**, 10–13.
6 R. S. Keri, A. Hiremathad, S. Budagumpi and B. M. Nagaraja, *Chem. Biol. Drug Des.*, 2015, **86**, 19–65.
7 K. Gobis, H. Foks, M. Serocki, E. Augustynowicz-Kopeć and A. Napiórkowska, *Eur. J. Med. Chem.*, 2014, **89**, 13–20.

8   K. Gobis, H. Foks, K. Suchan, E. Augustynowicz-Kopeć, A. Napiórkowska and K. Bojanowski, *Bioorg. Med. Chem.*, 2015, **23**, 2112–2120.

9   R. S. Keri, C. K. Rajappa, S. A. Patil and B. M. Nagaraja, *Pharmacol. Rep.*, 2016, **68**, 1254–1265.

10 P. Picconi, C. Hind, S. Jamshidi, K. Nahar, M. Clifford, M. E. Wand, J. M. Sutton and K. M. Rahman, *J. Med. Chem.*, 2017, **60**, 6045–6059.

11 L. Zhang, D. Addla, J. Ponmani, A. Wang, D. Xie, Y. N. Wang, S. L. Zhang, R. X. Geng, G. X. Cai, S. Li and C. H. Zhou, *Eur. J. Med. Chem.*, 2016, **111**, 160–182.

12 J. Löwe and L. A. Amos, *Nature*, 1998, **391**, 203–206.

13 T. K. Beuria, P. Singh, A. Surolia and D. Panda, *Biochem. J.*, 2009, **423**, 61–69.

14 E. L. White, *J. Antimicrob. Chemother.*, 2002, **50**, 111–114.

15 R. C. Reynolds, S. Srivastava, L. J. Ross, W. J. Suling and E. L. White, *Bioorg. Med. Chem. Lett.*, 2004, **14**, 3161–3164.

16 K. Kumar, D. Awasthi, S. Lee, I. Zanardi, B. Ruzsicska, S. Knudson, P. J. Tonge, R. A. Slayden and I. Ojima, *J. Med. Chem.*, 2011, **54**, 374–381.

17 J. Verma, V. M. Khedkar and E. C. Coutinho, *Curr. Top. Med. Chem.*, 2010, **10**, 95–115.

18 N. D. Sitwala, V. K. Vyas, B. C. Variya, S. S. Patel, C. C. Mehta, D. N. Rana and M. D. Ghate, *Bioorg. Chem.*, 2017, **75**, 118–126.

19 B. Park, D. Awasthi, S. R. Chowdhury, E. H. Melief, K. Kumar, S. E. Knudson, R. A. Slayden and I. Ojima, *Bioorg. Med. Chem.*, 2014, **22**, 2602–2612.

20 D. Awasthi, K. Kumar, S. E. Knudson, R. A. Slayden and I. Ojima, *J. Med. Chem.*, 2013, **56**, 9756–9770.

21 C. Yeh, C. Tung and C. Sun, *J. Comb. Chem.*, 2000, **2**, 341–348.

22 L. Chen, C. Chang, D. B. Salunke and C. Sun, *ACS Comb. Sci.*, 2011, **13**, 391–398.

23 S. Oda, H. Shimizu, Y. Aoyama, T. Ueki, S. Shimizu, H. Osato and Y. Takeuchi, *Org. Process Res. Dev.*, 2012, **16**, 96–101.

24 D. Ashok, S. Gundu, V. K. Aamate and M. G. Devulapally, *Mol. Diversity*, 2018, **22**, 769–778.

25 A. K. Chaturvedi, A. K. Verma, J. P. Thakur, S. Roy, S. Bhushan Tripathi, B. S. Kumar, S. Khwaja, N. K. Sachan, A. Sharma, D. Chanda, K. Shanker, D. Saikia and A. S. Negi, *Bioorg. Med. Chem.*, 2018, **26**, 4551–4559.

26 R. Ismail, T. S. Choon, A. C. Wei, M. A. Ali and Y. K. Yoon, *Eur. J. Med. Chem.*, 2013, **93**, 614–624.

27 T. Parish, T. R. Ioerger, A. Manning, J. Odingo, J. Sacchettini, T. O'Malley, P. A. Hipskind, D. Awasthi, N. S. Chandrasekera, L. Flint, T. Masquelin, B. J. Berube, G. Shetye and S. Chettiar, *ACS Infect. Dis.*, 2017, **3**, 898–916.

28 C. Chhotaray, M. M. Islam, H. M. A. Hameed, Z. Liu, T. Zhang, M. Hussain, Z. Lu, Y. Gao and G. Surineni, *MedChemComm*, 2018, **10**, 49–60.

29 S. Ahamad, A. Islam, F. Ahmad, N. Dwivedi and M. I. Hassan, *Comput. Biol. Chem.*, 2019, 0–1.

30 H. Akamatsu, K. Fukase and S. Kusumoto, *J. Comb. Chem.*, 2002, **4**, 475–483.

31 C. Chen, M. Chien, M. Kuo, C. Chou, J. Lai, S. Lin, S. Thummanagoti, C. Sun and R. V. June, *J. Comb. Chem.*, 2009, **11**, 1038–1046.

32 J. Ramprasad, N. Nayak, U. Dalimba, P. Yogeeswari, D. Sriram, S. K. Peethambar, R. Achur and H. S. S. Kumar, *Eur. J. Med. Chem.*, 2015, **95**, 49–63.

33 K. Chaudhari, S. Surana, P. Jain and H. M. Patel, *Eur. J. Med. Chem.*, 2016, **124**, 160–185.

34 J. Lalut, B. B. Tournier, T. Cailly, M. Since, P. Millet, S. Corvaisier, A. Davis, C. Ballandonne, F. Fabis, P. Dallemagne and C. Rochais, *Eur. J. Med. Chem.*, 2016, **116**, 90–101.

35 L. Wadsö and O. J. Karlsson, *Polym. Degrad. Stab.*, 2013, **98**, 73–78.

36 S. Kidwai, C.-Y. Park, S. Mawatwal, P. Tiwari, M. G. Jung, T. P. Gosain, P. Kumar, D. Alland, S. Kumar, A. Bajaj, Y.-K. Hwang, C. S. Song, R. Dhiman, I. Y. Lee and R. Singh, *Antimicrob. Agents Chemother.*, 2017, **61**, e00969-17.